

A Jumping Robot Using Soft Pneumatic Actuator

Feng Ni, *Student Member, IEEE*, Daniel Rojas, Kai Tang*, Lilong Cai, *Member, IEEE*, Tamim Asfour, *Member, IEEE*

Abstract— This paper presents the development of a new type of robot capable of vertical and directional jumping. The robot uses soft silicone elastomer based pneumatic actuators as legs that accelerate the platform upwards by rapid pressurization. The robot is able to control and adjust the direction of the jumping by altering the timing patterns in which the individual legs are activated.

I. INTRODUCTION

Locomotion has become a popular research area in robotics. Traditional terrestrial locomotion techniques such as wheeled locomotion and many legged designs encounter large difficulty when facing challenges such as uneven terrain and high obstacles. In order to enable these mechanisms to prevail in these situations, more complexity must be added to the robot configuration and structure.

A very promising approach for robot locomotion to efficiently overcome obstacles is to fly over them [1]. Comparing to relative low energy efficiency of continuous flight, jumping has been adopted widely by small animals in nature to overcome large obstacles [2].

Jumping is a form of locomotion in which a mechanical system propels itself into the air along a ballistic trajectory. A broad overview on jumping robot is provided by Armour et al. [1], while the basic physics of jumping is given by Dufresne et al. [3]. As always, bio-inspiration becomes an apt solution for robotic designs: be it frogs [4], fleas [5] or kangaroos [6], the animal kingdom provides a plethora of mechanisms and strategies.

Jumping abilities can also be combined with traditional wheeled [7, 8] or walking modes [9, 10] to increase compatibility. Here, the robot's capabilities are extended by the jumping mode with regards to traversing rough terrain and overcoming obstacles, while others rely on jumping as the sole strategy for locomotion.

Most jumping robot designs lock energy in a spring or similar devices via a locking mechanism [11-13] and release the energy drastically to propel the robot upwards/forwards. There are some noticeable exceptions with energy store and release, such as using a jet of air by Kim et al. [14], the "closed elastica" proposed by Yamada et al. [15], and the deforming elastic ring by Suguyama et al. [16]. Since the flight of these very light robots is often unstable, self-recovery capabilities have been used in many cases [2, 17, 18]. Applications

proposed by Burdick and Fiorini [19] show the prospective major role of jumping robot where the constraints set by gravitation are less on Earth.

Jumping has also be merged with gliding to obtain higher system efficiency as well as to solve the problem of landing. A robot composed of a couple of four-bar mechanisms to support both jumping and gliding is developed by Woodward et al [28]. A functional model of a simple jump-glider combined locomotion is built and verified by Desbiens et al [29] with visionary design choices and control strategies.

Soft robots, structured and actuated by compliant and deformable materials, are an emerging research field to achieve robotic functionality. Getting rid of complicated mechanical structures to function, soft robots achieve complex movements from the characteristics of the material itself; combined with a specialized morphology, they reduce the number of individual parts and increase the robustness. Some research in soft robotics has already dealt with developing systems for object grasping [20, 21] and bio-inspired locomotion [22, 23].

So far, only limited exploration has been made to merge controllable jumping with soft robotics. A novel design of jumping soft robot powered by an inner explosion was proposed by Shepherd [24], followed by a new version developed by Tolley [27] that is able to control the jumping direction by varying the configuration.

However, as for a mobile pneumatic system, it is still not efficient enough using pressurized gas to change configuration for direction control. To avoid extra power consumption and structural redundancy for a directional jumping, a robot platform using soft pneumatic actuators that reply on quick variation of orientation to perform directional jumping is presented here.

The principle of understanding-by-building by Pfeifer et al. [25] guides the development of our robot, from concept to a working prototype. Section II describes the design and tests of the soft actuator on its static/dynamic performance. Mechanisms of vertical and directional jumping are illustrated and verified in Section III, along with the implementation of a control method to adjust the deviation along the intended jumping direction. Section IV gives the summary and outlook on further investigation.

This work is supported by the Hong Kong Innovation & Technology Fund. F. Ni, K. Tang, L. Cai are with the Department of Mechanical and Aerospace Engineering, Hong Kong University of Science and Technology, Hong Kong. (*Corresponding author: Dr. Kai Tang, mektang@ust.hk).

D. Rojas and T. Asfour are with the High Performance Humanoid Technologies Lab, Institute for Anthropomatics and Robotics, Karlsruhe Institute of Technology, Germany (e-mail: mail@danielrojas.net).

II. SOFT ACTUATOR

The soft actuator presented in this section is used as the leg of jumping robot. In the following chapters, the design of the actuator is described. Actuator's static and dynamic behavior are presented as a preliminary prediction of its performance on the robot platform.

A. Design

The overall shape of the soft actuator is shown in Fig. 1. It is designed based on a resemblance to the bending actuators used as ARMAR III's palm and finger joints [26].

From top down (Fig. 1B.1), it starts with a neck that allows for easy mounting onto a platform or testing jig. By inserting it into a hole with a slightly smaller diameter than the neck itself, a tight fit is ensured and then further reinforced by the insertion of the air supply pipe. There is no leakage within the design up to 0.15 MPa static and 0.6 MPa in bursts of up to 50 ms. With the neck as inlet on the top, the body of the actuator is comprised of two circular discs joined at the outer perimeter (Fig. 1B.2), thus creating the air chamber. Fig. 1C shows the state when the actuator is not pressurized and Fig. 1D shows its state of expanding outwards when pressurized.

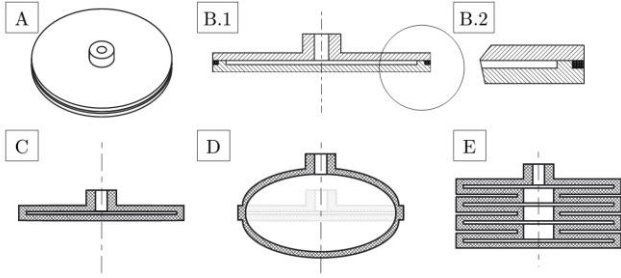


Figure 1 – an overview of the soft actuator

The effective diameter of the inner chamber is designed to be 50 mm and the thickness of the actuator is 1mm to compromise between manufacturing convenience and reasonable internal volume, as larger actuators would require a much higher flow rate to reach the same rate of expansion.

A multi-segment actuator (Fig. 1E) is also developed. Following the same basic structure, the individual segments are joined by smaller rings. The modular design allows for stacks of an arbitrary number of segments.

ShinEtsu KE-1310ST is chosen to make the soft actuator for its good material properties. It is able to withstand a wider range of pressure and is chemically convenient to handle.

B. Static behavior of the actuator

Static tests are conducted to characterize the static force F exerted by the actuator at different degrees of inflation s under a given internal air pressure p . A test jig (Fig. 2) is designed and various tests are carried out to model the behavior of actuator as $F = f(s, p)$.

Assumptions are made to approximate the results of test:

- The initial force at $s = 0$ is assumed to be proportional to the internal pressure following the pressure law ($F = pA$) and reduced by an efficiency factor representing unconsidered effects.

$$F_{\max}(p) = CpA \quad (1)$$

The data later obtained support this assumption well.

- The maximum achievable expansion at a given pressure $s_{\max}(p)$ is assumed to follow a linear pattern, with a certain offset from a proportional behavior.

$$s_{\max}(p) = Vp + W \quad (2)$$

A quadratic model of static force is created based on these two assumptions.

$$F(s, p) = Xs^2 + Ys + Z \quad (3)$$

While X, Y, Z can be obtained by the following boundary conditions:

- When the maximum force is achieved at zero expansion:

$$F(s = 0, p) = F_{\max}(p) \quad (4)$$

- When the actuator fully expands and exerts no force:

$$F(s = s_{\max}(p), p) = 0 \quad (5)$$

- The force diminishes smoothly up to the actuator's full expansion:

$$\frac{\partial F}{\partial s}(s = s_{\max}(p), p) = 0 \quad (6)$$

For the first test, the actuator is allowed to expand along its axis between $0 \text{ mm} < s < 20 \text{ mm}$, by a 0.5 mm increment. At each position, the pressure is increased to a maximum of 80 kPa in 10 kPa steps, and the force is measured after a brief period of stabilization. This included a measurement at $p = 0$ kPa at every position s to improve the accuracy and compensate for a possible drift in the sensor output. The test allowed plotting complete curves for lower pressures up to 30 kPa, from $0 \text{ mm} < s < s_{\max}$, which is the maximum possible expansion when the actuator eventually stops touching the sensor plate.

The measured force at $s = 0$ is found to be 50% to 62% of the theoretical maximally reachable force ($F = pA$, whereas A is the contact area between the actuator and load cell), with higher ratios achieved at higher pressures. The force over expansion ratio for a specific pressure ($F = (s, p = \text{const})$) appears to follow a quadratic trend, with the minimum point being reached at $s = s_{\max}$.

A second series of tests is conducted using a version of the sensor capable of measuring load of up to 20 kg, eliminating the previous limitations. Pressure of up to 160 kPa could now be measured from $s = 0$.

Since the expected trend of the curves is already known, the pressure step is doubled to 20 kPa and the expansion increment increased to 2 mm. With the current setup, displacement up to $s = 22 \text{ mm}$ can be recorded. Also, the actuator failed at $p = 140 \text{ kPa}$ and $s = 22 \text{ mm}$.

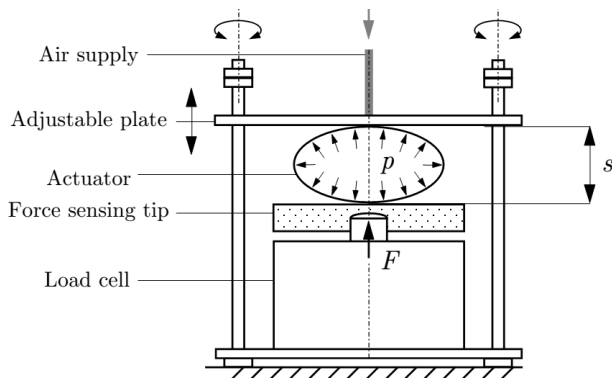


Figure 2 – static test bed

The obtained curves are a good approximation for the measured data points, often resulting in a more conservative estimate of the achievable force than what is actually measured (dashed lines in Fig. 3).

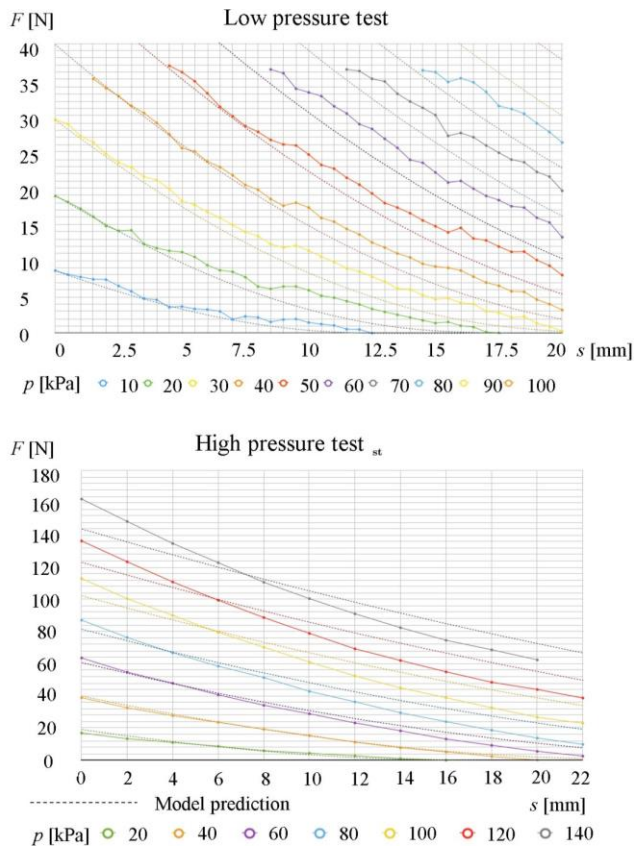


Figure 3 – static test results

C. Dynamic behavior of the actuator

Instead of building a prototype robot for preliminary test, to simulate jumping, the soft actuator is given a sudden burst of pressure to launch a mass (much heavier than the actuator itself) on top of it into the air. The mass launched is supposed to act as the robot mass shared by a single actuator during the jumping.

Fig. 4 shows the experiment setup. A valve is opened to generate a burst of pressure into the actuator and the same pulse triggers a high speed camera to record the actuator's expansion process. Markers for vision tracking are placed on

the actuator and the payload respectively so that their trajectories can be recognized and tracked. Totally 27 tests are performed, with pressure ranging from 0.1 to 0.4 MPa and loads up to 0.106 kg, including a series with no additional payload. For each run, the maximum height that the payload mass reaches is recorded.

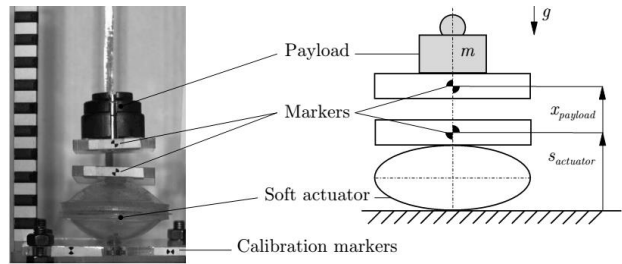


Figure 4 – dynamic test bed

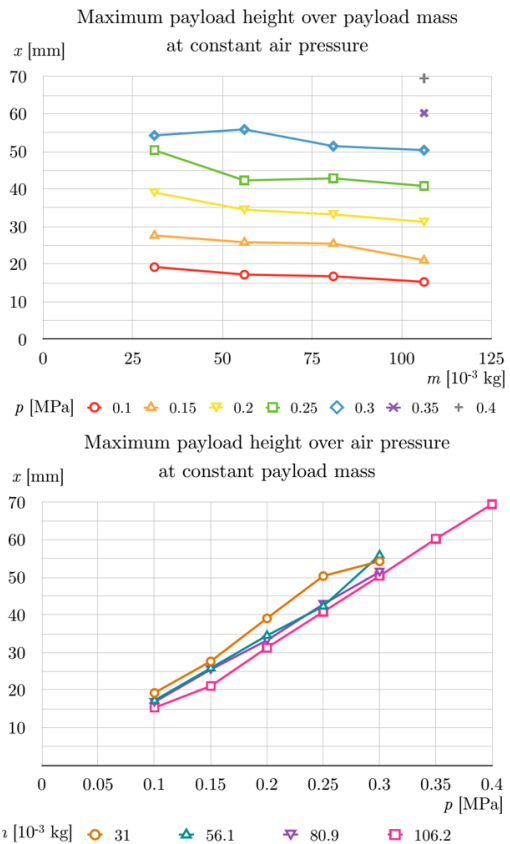


Figure 5 – dynamic test result: jumping height over payload weight and input pressure

The relationship between the payload mass and the maximum jumping height is graphed under different air pressures, along with the jumping height over the applied air pressure being plotted for each payload used (Fig. 5). The maximum reached height relates linearly to the applied air pressure, declining only slightly as the mass of the payload increases. A detailed mathematical description will be established as an important future work to understand this interesting phenomenon.

III. THE JUMPING ROBOT

This section reports our jumping robot design. The proposed mechanisms of vertical jumping and directional

jumping are explained respectively first, followed then by the description of the implementation details and the evaluation of an effective control methodology for adjusting the direction of jumping.

A. Design

Fig. 6 shows the configuration of our robot platform. The central piece of the robot's structure is an acrylic sheet (5mm thickness). Each one of the four legs holds an actuator on its end, whose actuation is controlled by a solenoid valve. Due to the pipe layout constraint, the valve on one leg controls the actuator of the next leg, circling clockwise in the top view. Sitting in the middle of the platform is the core electronics and air distribution module.

B. Vertical jumping

Observation from our previous dynamic tests indicates the feasibility of vertical jumping. In the previous tests, the payload is found to separate from the actuator before 50 ms (Fig. 6). Therefore, the actuation time of the valves is set to 50 ms for all the tests on the robot to guarantee a full acceleration phase, while preventing rupture of the actuator. The pressure is set to 0.5 MPa to determine the maximum achievable jumping height. High speed camera is used to record/measure the height.

The test jumps averaged a height of 95 mm under pressure of 0.5 MPa (Fig. 7), with variations of approx. ± 5 mm over the five measured jumps. This more or less matches the prediction made from the previous dynamic tests (which would have yielded around 88 mm assuming an average load of $\frac{1}{4}m = 180g$ per leg at 0.5 MPa).

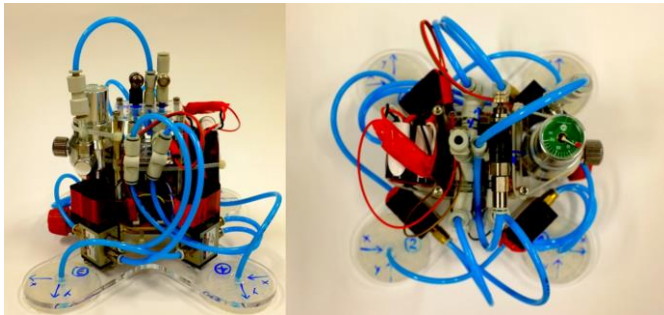


Figure 6 – front view and over view of the robot platform

Quite possibly, performance is stifled due to energy loss inside the pneumatic system. The combination of the pressure regulator and the 4 mm pipes connecting the components and the multiple T-joints puts limit on the amount of air that enters the actuators during the acceleration period, thus reducing the energy efficiency.

It was noticed that the experiment that works well using only one actuator would encounter problems once four legs have to be actuated at the same time. The comparison between the jumping performance and the tests conducted with a single actuator should not be taken as an absolute measure, as different valves and slightly improved actuators are used in the final prototype. A further investigation of the fluid dynamic and rheological effects inside the system will be conducted in the future. Nevertheless, some basic conclusions on the general behavior of the platform can be made at this stage.

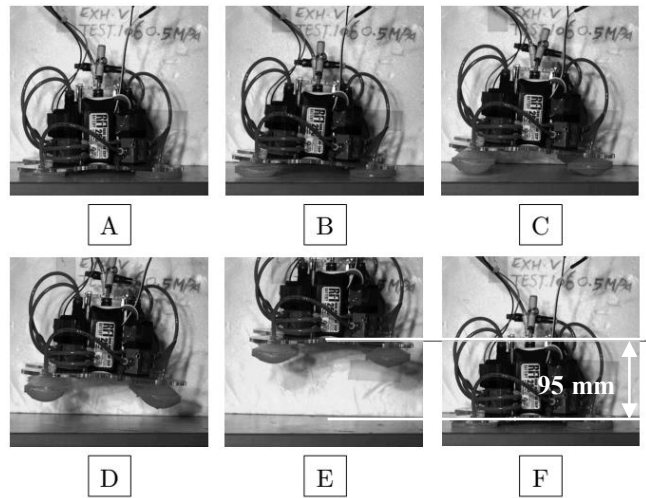


Figure 7 – vertical jumping test of the jumping robot

C. Directional jumping

Using the developed robot platform, we designed and fabricated a mechanism to generate a directional jump based on the concept of relying on different timing patterns to actuate the four legs, as presented next.

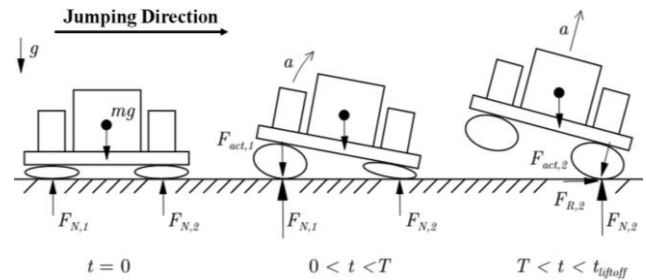


Figure 8 – directional jumping concept

The mechanism is illustrated in Fig. 8. By initially inflating the rear legs (defined as the actuators opposite the direction of the intended heading, from the platform's center) first, the entire rear section of the robot is pushed upwards into the air while the front legs are still inactive and remain on the ground, causing the robot to rotate along its sideways axis (achieving a negative pitch when described in roll-pitch-yaw coordinates). A subsequent inflation of the front legs (now tilted relative to the ground) would yield a force separating into a constituent normal to the ground, reversing the pitching motion of the platform and propelling it further into the air, and a tangential force (caused by friction) effectively pushing the entire robot forward before lifting off. Depending on the parameters of the experiment, the platform may or may not reach a horizontal position (pitch = 0) in the air before touching down again. The result recorded by the camera fits the purposed concept well (Fig. 9), which can be also observed in the companion multimedia attachment.

To find timing patterns maximizing a single jump distance, a series of tests is performed. The delay in activation between the front and rear legs' solenoids is incrementally adjusted in each test ranging from 10 ms to 100 ms with a 10 ms increment. Afterwards, the platform's position is measured relative to the starting point. The experiment is repeated to observe the differences caused by unknown facts.

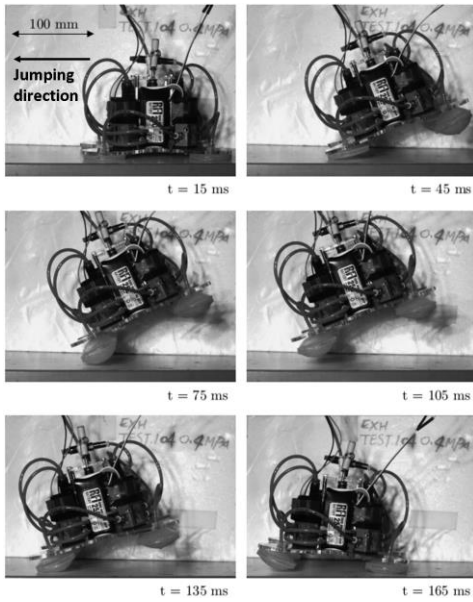


Figure 9 – recorded directional jumping process

From the measured positions of the robot, its deviation from a straight trajectory, and its yaw angle are calculated and plotted in Fig. 10. Each color represents the test series in a certain direction. Fig. 10 also shows the results of every single run and the average over five runs. The x-axis displays the actuation delay between the rear and front legs, in ms.

D. Direction adjustment control

Most of the tests show significant sideways drifting of the robot to either side, deviating from the intended heading while simultaneously rotating (Fig. 12A).

It was observed that at times, an actuator showing subpar performance due to slower expansion would have different effects on the platform jumping behavior. Intuitively, a difference between the two rear actuators causes only small deviations, whereas the robot would noticeably swerve towards one side of the weaker leg when the defect is on a front actuator. This is confirmed by artificially “weakening” one of the front legs through delaying its actuation time by an interval d than the other legs. Even delays in the order of $1 \text{ ms} \leq d \leq 3 \text{ ms}$ are observed to change heading of 10° .

This led to the development of a simple, proof-of-concept control strategy to help the robot maintain a straight heading by compensating for small deviations, as outlined in Fig. 11. After performing a (theoretically) straight jump, the compass sensor would measure any change in heading and adjust the timing pattern accordingly before continuing with the next jump.

The primitive solution presented here takes the deviation $\Delta\alpha_i$ gathered by the sensor (in degrees) after the i th jump, and determines a new delay d_i based on the delay used in the previous jump d_{i-1} and the deviation $\Delta\alpha_i$ scaled by a learning rate factor μ . Depending on the sign of d_i , either the left or right front leg’s actuation is delayed by the amount $d_{1,i}$ or $d_{2,i}$, respectively (Fig. 11).

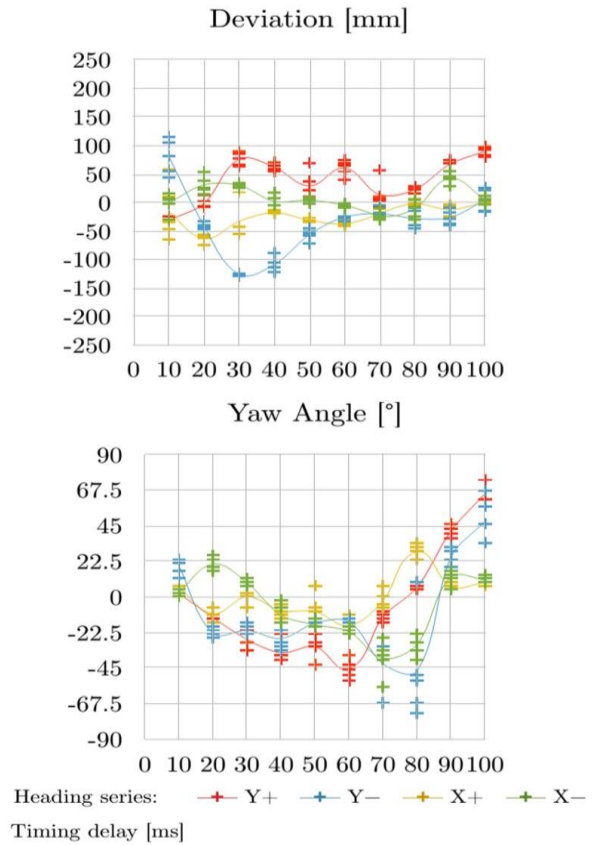


Figure 10 – directional jumping test data

$$d_0 = 0 \quad (7)$$

$$d_i = d_{i-1} + \mu \cdot \Delta\alpha_i \quad (8)$$

$$d_{1,i} = \begin{cases} |d|, & \text{if } d_i < 0 \\ 0, & \text{otherwise} \end{cases} \quad (9)$$

In practice, a factor of $\mu = 1$ (adjusting delay by 1 ms for 1 degree of deviation) proved to be most proficient, as higher values would result in an overcorrecting and zigzag motion. Rotational deviation can be effectively compensated for by this method as well.

By continually tuning the jumping parameters, this resulted in a proportional control scheme able to dramatically improve the locomotion performance (Fig. 12B). The effect of direction control can be observed in the companion video in the multimedia attachment.

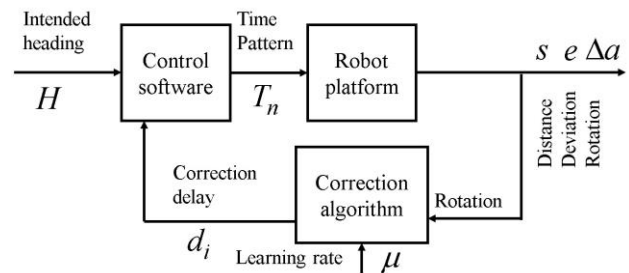


Figure 11 – control strategy for compensating angle deviation

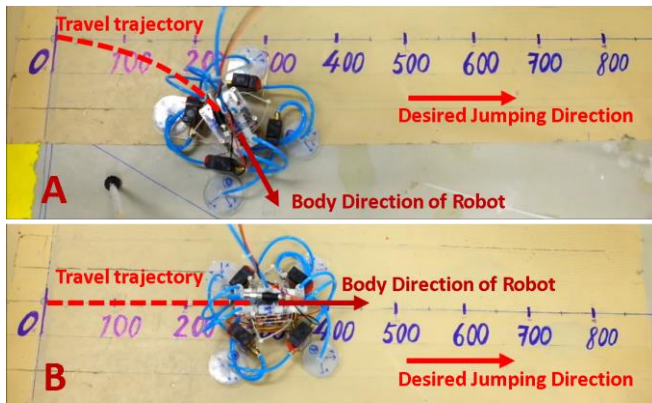


Figure 12 – the heading direction before (A) and after (B) control is applied

IV. CONCLUSION

In this paper, the development of a new type of jumping robot is reported, starting from the conceptual design of the soft actuator all the way to a working prototype. The directional jumping based on time patterning is proven to be simple and effective. The proposed direction adjustment method that adapts the control parameters ensures the deviation from the intended path to stay as small as possible, which is also verified by the test results.

Future work includes modeling the dynamic behavior of the soft actuator and optimizing the actuator design. Theoretical model of directional jumping will also be established to achieve a better performance.

REFERENCE

- [1] R. Armour, K. Paskins, A. Bowyer, J. Vincent and W. Megill, "Jumping robots: a biomimetic solution to locomotion across rough terrain," *Bioinspiration & Biomimetics*, vol. 2, pp. S65, 2007.
- [2] M. Kovač, M. Schlegel, J. Zufferey and D. Floreano, "Steerable miniature jumping robot," *Autonomous Robots*, vol. 28, pp. 295-306, 2010.
- [3] R. J. Duffresne, W. J. Gerace and W. J. Leonard, "Springbok: the physics of jumping," *The Physics Teacher*, vol. 39, pp. 109-115, 2001.
- [4] M. Wang, X. Zang, J. Fan and J. Zhao, "Biological jumping mechanism analysis and modeling for frog robot," *Journal of Bionic Engineering*, vol. 5, pp. 181-188, 2008.
- [5] U. Scarfogliero, C. Stefanini and P. Dario, "Design and development of the long-jumping," in *Robotics and Automation, 2007 IEEE International Conference On*, 2007, pp. 467-472.
- [6] N. Carlési and A. Chemori, "Nonlinear model predictive running control of kangaroo robot: A one-leg planar underactuated hopping robot," in *Intelligent Robots and Systems (IROS), 2010 IEEE/RSJ International Conference On*, 2010, pp. 3634-3639.
- [7] K. Kikuchi, K. Sakaguchi, T. Sudo, N. Bushida, Y. Chiba and Y. Asai, "A study on a wheel-based stair-climbing robot with a hopping mechanism," *Mechanical Systems and Signal Processing*, vol. 22, pp. 1316-1326, 2008.
- [8] H. Tsukagoshi, M. Sasaki, A. Kitagawa and T. Tanaka, "Jumping robot for rescue operation with excellent traverse ability," in *Advanced Robotics, 2005. ICAR'05. Proceedings., 12th International Conference On*, 2005, pp. 841-848.
- [9] F. Kikuchi, Y. Ota and S. Hirose, "Basic performance experiments for jumping quadruped," in *Intelligent Robots and Systems, 2003. (IROS 2003). Proceedings. 2003 IEEE/RSJ International Conference On*, 2003, pp. 3378-3383.
- [10] A. M. Johnson and D. E. Koditschek, "Toward a vocabulary of legged leaping," in *Robotics and Automation (ICRA), 2013 IEEE International Conference On*, 2013, pp. 2568-2575.
- [11] U. Scarfogliero, C. Stefanini and P. Dario, "A bioinspired concept for high efficiency locomotion in micro robots: The jumping robot grillo,"

- in *Robotics and Automation, 2006. ICRA 2006. Proceedings 2006 IEEE International Conference On*, 2006, pp. 4037-4042.
- [12] M. Kovac, M. Fuchs, A. Guignard, J. Zufferey and D. Floreano, "A miniature 7g jumping robot," in *Robotics and Automation, 2008. ICRA 2008. IEEE International Conference On*, 2008, pp. 373-378.
- [13] J. Zhao, J. Xu, B. Gao, N. Xi, F. J. CINTRÓN, M. W. Mutka and L. Xiao, "MSU Jumper: a single-motor-actuated miniature steerable jumping robot," *Robotics, IEEE Transactions On*, vol. 29, pp. 602-614, 2013.
- [14] D. H. Kim, J. H. Lee, I. Kim, S. H. Noh and S. K. Oho, "Mechanism, control, and visual management of a jumping robot," *Mechatronics*, vol. 18, pp. 591-600, 2008.
- [15] A. Yamada, M. Watari, H. Mochiyama and H. Fujimoto, "An asymmetric robotic catapult based on the closed elastica for jumping robot," in *Robotics and Automation, 2008. ICRA 2008. IEEE International Conference On*, 2008, pp. 232-237.
- [16] Y. Sugiyama and S. Hirai, "Crawling and jumping by a deformable robot," *The International Journal of Robotics Research*, vol. 25, pp. 603-620, 2006.
- [17] M. Kovac, M. Schlegel, J. Zufferey and D. Floreano, "A miniature jumping robot with self-recovery capabilities," in *Intelligent Robots and Systems, 2009. IROS 2009. IEEE/RSJ International Conference On*, 2009, pp. 583-588.
- [18] J. Zhao, R. Yang, N. Xi, B. Gao, X. Fan, M. W. Mutka and L. Xiao, "Development of a miniature self-stabilization jumping robot," in *Intelligent Robots and Systems, 2009. IROS 2009. IEEE/RSJ International Conference On*, 2009, pp. 2217-2222.
- [19] J. Burdick and P. Fiorini, "Minimalist jumping robots for celestial exploration," *The International Journal of Robotics Research*, vol. 22, pp. 653-674, 2003.
- [20] E. Brown, N. Rodenberg, J. Amend, A. Mozeika, E. Steltz, M. R. Zakin, H. Lipson and H. M. Jaeger, "Universal robotic gripper based on the jamming of granular material," *Proceedings of the National Academy of Sciences*, vol. 107, pp. 18809-18814, 2010.
- [21] F. Ilievski, A. D. Mazzeo, R. F. Shepherd, X. Chen and G. M. Whitesides, "Soft robotics for chemists," *Angewandte Chemie*, vol. 123, pp. 1930-1935, 2011.
- [22] R. F. Shepherd, F. Ilievski, W. Choi, S. A. Morin, A. A. Stokes, A. D. Mazzeo, X. Chen, M. Wang and G. M. Whitesides, "Multigait soft robot," *Proc. Natl. Acad. Sci. U. S. A.*, vol. 108, pp. 20400-20403, Dec 20, 2011.
- [23] B. A. Trimmer, A. E. Takesian, B. M. Sweet, C. B. Rogers, D. C. Hake and D. J. Rogers, "Caterpillar locomotion: A new model for soft-bodied climbing and burrowing robots," in *7th International Symposium on Technology and the Mine Problem*, 2006, pp. 1-10.
- [24] R. F. Shepherd, A. A. Stokes, J. Freake, J. Barber, P. W. Snyder, A. D. Mazzeo, L. Cademartiri, S. A. Morin and G. M. Whitesides, "Using explosions to power a soft robot," *Angewandte Chemie*, vol. 125, pp. 2964-2968, 2013.
- [25] D. I. Poole, R. G. Goebel and A. K. Mackworth, *Computational Intelligence*. Oxford University Press Oxford, 1998.
- [26] I. Gaiser, S. Schulz, A. Kargov, H. Klosek, A. Bierbaum, C. Pylatiuk, R. Oberle, T. Werner, T. Asfour and G. Bretthauer, "A new anthropomorphic robotic hand," in *Humanoid Robots, 2008. Humanoids 2008. 8th IEEE-RAS International Conference On*, 2008, pp. 418-422.
- [27] M. T. Tolley, R. F. Shepherd, M. Karpelson, N. W. Bartlett, K. C. Galloway, M. Wehner, R. Nunes, G. M. Whitesides and R. J. Wood, "An untethered jumping soft robot," in *Intelligent Robots and Systems (IROS 2014), 2014 IEEE/RSJ International Conference on*, 2014, pp. 561-566.
- [28] M. A. Woodward and M. Sitti, "Design of a miniature integrated multi-modal jumping and gliding robot," in *Intelligent Robots and Systems (IROS), 2011 IEEE/RSJ International Conference on*, 2011, pp. 556-561.
- [29] A. L. Desbiens, A. T. Asbeck and M. R. Cutkosky, "Landing, perching and taking off from vertical surfaces," *The International Journal of Robotics Research*, pp. 0278364910393286, 2011.